ELSEVIER

Sensors and Actuators 80 (2000) 23–30

SENSORS AND ACTUATORS A PHYSICAL

www.elsevier.nl/locate/sna

A piezoelectric tactile sensor with three sensing elements for robotic, endoscopic and prosthetic applications

J. Dargahi *

School of Engineering Science, Simon Fraser University, Burnaby, BC, Canada V5A 1S6

Received 5 June 1998; received in revised form 20 August 1999; accepted 2 October 1999

Abstract

This paper reports on a prototype tactile sensing system with only three sensing elements. The magnitude and position of the applied force is obtained by utilising triangulation approach combined with membrane stress. Some information about the shape of the contacted object is obtained. The polyvinylidene fluoride (PVDF) sensor is designed to overcome the problems of cross talk between sensing elements and to reduce the complexity associated with some PVDF tactile sensors arranged in matrix form. A theoretical analysis of the sensor is made and compared with experimental results. The limitation of the sensor is also reported. The sensor in miniaturised form can also be integrated into an endoscopic grasper and a prosthetic finger. © 2000 Elsevier Science S.A. All rights reserved.

Keywords: Tactile sensor; Robotics; Prosthetics; Endoscopic surgery; Polyvinylidene fluoride; Piezoelectric; Cross talk; Sensing element

1. Introduction

The fundamental requirements of future competent robotic tactile sensors are the capability of determining the magnitude of the applied force and identifying its position on the surface of the tactile sensor [1,26]. To achieve these requirements, most investigators have attempted to design tactile sensors with a number of discrete sensing elements arranged in matrix form [2,3,5–11,18]. When a force is applied to a sensing element of a matrix tactile sensor, an undesirable response from the nearest neighbour sensing elements (cross talk) often occurs leading to error in measurements. Where polyvinylidene fluoride (PVDF) film is used to design a matrix of high spacial resolution tactile sensors, these problems are often reported [1,3,5,12–14]. In addition to the problem of cross talk, complexity and fragility is also reported. In many designs of tactile sensors, the PVDF is often supported by a rigid substrate [2–4,6]. These sensors, however, require a compliant layer to avoid damage to the object in contact. The problem with this approach is that the effect of the applied force spreads over the adjacent sensing elements, thus increasing the cross talk [6]. However, some design approaches are reported to reduce this problem [1]. As there is very little deformation of the PVDF film under compressive stress on a rigid substrate, the sensing element produces only a small electric charge when it is compressed. One solution is to increase the sensitivity by backing the PVDF film with an elastomer sheet. As a result, the applied contact force induces membrane stress in the PVDF film and substantially increases the output electrical signal. This is done, however, at the expense of the sensor's spacial resolution, because in a matrix array of PVDF sensing elements, an applied force on a single sensing element would produce large strains and correspondingly large signals in the contiguous sensing elements [12]. In addition, due to the capacitative nature of PVDF sensing elements, electrical interference may occur due to inter-electrode capacitance between the adjacent sensing elements; however, this is likely to be insignificant. A further problem with the matrix array of PVDF sensing elements is that, it requires one coaxial cable for each sensing element. The microminiature coaxial cables, of outer diameter between 0.6 and 2 mm, form a bundle whose size and poor flexibility represent an additional limitation [1]. The increase in the number of sensing elements also increases the number of connection points, leading to sensor fragility.

In this paper, a membrane tactile sensing system with only three sensing elements is designed. By utilising the membrane stress combined with a triangulation method, it is shown that tactile sensing can be achieved in a system where the above problems are not manifested.

* E-mail: dargahi@cs.sfu.ca

PII: S0924-4247(99)00295-2

Section 1.1 describes the fundamentals of PVDF film in relation to tactile sensing. Section 2 reports on the triangulation approach used on the membrane PVDF sensor. The experimental measurements presented are for a three-element membrane tactile sensing system and this is presented in Section 3. Section 4 is devoted to theoretical analysis of the membrane system, and the overall discussion is conducted in Section 5.

1.1. Fundamentals of PVDF film

PVDF is a semicrystalline polymer of approximately 50%–65% crystallinity. The polymer consists of long chain molecules with repeated unit CF_2–CH_2. The reason for the strong piezo-pyroelectric activity is related to the large electronegativity of fluoride atoms in comparison to the carbon atoms, thus accommodating a large dipole moment.

The beta phase of PVDF forms a crystal symmetry of C_{2v} [15,20]. The piezoelectric coefficient for this form is shown as:

$$d_{ij} = \begin{vmatrix} 0 & 0 & 0 & 0 & d_{15} & 0 \\ 0 & 0 & 0 & d_{24} & 0 & 0 \\ d_{31} & d_{32} & d_{33} & 0 & 0 & 0 \end{vmatrix}$$

The axes used are defined in terms of the draw direction (direction 1), normal to the draw direction in the plane of the film (direction 2) and normal to the plane of the film (direction 3). This is shown in Fig. 1. For the biaxially oriented beta form of PVDF, the crystal symmetry is $c_{\infty v}$, which implies a similar d_{ij} coefficient matrix to that of uniaxially oriented PVDF, except that $d_{31} = d_{32}$ and $d_{15} = d_{24}$.

The sensitivity of uniaxially oriented PVDF film is dependent on the direction of measurement, that is, drawn, transverse or thickness. When a tensile force is applied in the drawn direction (1–1) (see Fig. 1), the output charge is expressed by:

$$\frac{Q}{A_3} = d_{31}\frac{F}{A_1} = d_{31}\sigma_1. \tag{1}$$

Similarly, the output charge due to stress in the transverse direction (2–2) is expressed by:

$$\frac{Q}{A_3} = d_{32}\frac{F}{A_2} = d_{32}\sigma_2, \tag{2}$$

where Q is the output charge, A_3 is the electroded area of the PVDF film, A_1 and A_2 are the cross-sectional areas of the film perpendicular to the direction of the applied force, d_{31} is the piezoelectric strain coefficient in the drawn direction, d_{32} is the piezoelectric strain coefficient in the transverse direction, F is the applied force, σ_1 is the applied tensile stress in the drawn direction and σ_2 is the applied tensile stress in the transverse direction.

When a PVDF film is compressed by a probe on a rigid flat surface, assuming, that both the flat surface and the probe are friction-free, the film is free to expand laterally, that is, in the 1–1 and 2–2 directions; since then $Q/A_3 = d_{33}(F/A_3)$, the output charge can be expressed as:

$$Q = d_{33}F, \tag{3}$$

where d_{33} is the piezoelectric strain coefficient in the 3–3 direction.

Normally, friction does exist and, moreover, in tactile sensing, the PVDF film is frequently glued to a rigid substrate. In this condition, the output charge is due to a combination of d_{31}, d_{32} and d_{33}. It is interesting to note that, for a given applied force, the output charge from the film in the lateral direction is much higher than that of thickness direction. This is because of the extreme thinness of the PVDF film, which results in much higher stresses being applied to the film (see Eqs. (1) and (2)). For PVDF film, d_{31} and $d_{32} > 0$, $d_{33} < 0$ and $-d_{33} \geq d_{31} > d_{32} > 0$. For the commercially available uniaxially oriented PVDF film, the values of d_{31} and d_{32} are normally of the order of 20 and 2 pC/N, respectively.

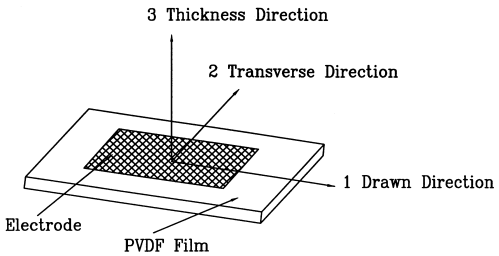

Fig. 1. Schematic picture of a PVDF film showing the conventional identification of the axes. The 1, 2, 3 directions represent the drawn, transverse and thickness direction of the film, respectively.

2. Triangulation approach on membrane PVDF sensor

The identification of a point on a 2-D plane requires the value of its coordinates to be known. The position of a point on the plane can be found from knowledge of its distance from three reference points whose coordinates are known. The need for the distances from three reference points whose coordinates are known can easily be seen by considering the case where the distances from only two reference points are known. These distances define a circle about each of the reference points, and their intersection gives the position of the unknown point. There are, however, two intersections so that these distances do not unambiguously define the position of the unknown point. This is shown in Fig. 2 and demonstrated below, where it is shown that for a two-reference point system, the coordinate of the unknown point is determined by the solution of a quadratic equation.

$$r_a^2 = (x_a - x_p)^2 + (y_a - y_p)^2, \tag{4a}$$

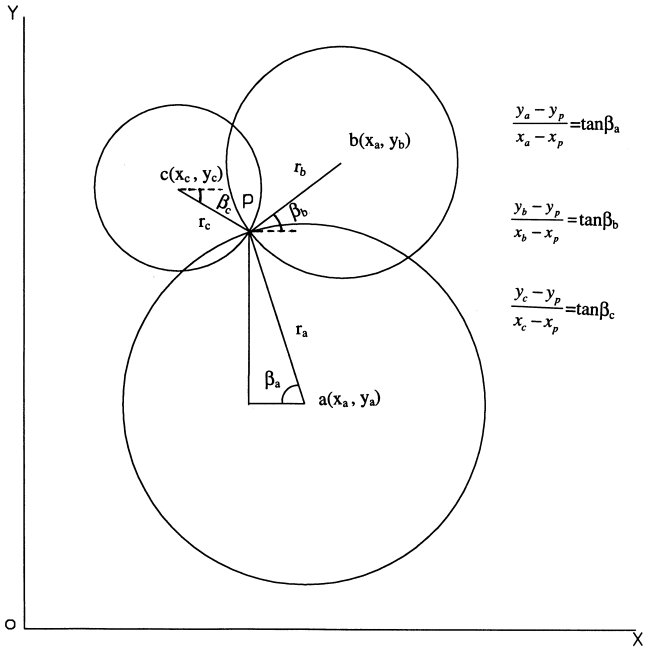

Fig. 2. The three circles with radii r_a, r_b and r_c, showing that the location of any point, on the 2-D plane, can be obtained from a knowledge of the distance from three points whose positions are known.

similarly

$$r_b^2 = (x_b - x_p)^2 + (y_b - y_p)^2 \quad (4b)$$

$$r_c^2 = (x_c - x_p)^2 + (y_c - y_p)^2. \quad (4c)$$

Solving Eqs. (4a) and (4b) for x_p and y_p gives a quadratic equation. When a third reference point is added, the position of the known point can be unambiguously determined by linear equations, as it will eliminate one of the possible positions.

When PVDF is used in a membrane mode and a point force is applied, the membrane stresses can be used to define the distance from a number of sensing elements in the surface of the membrane. When three sensing elements (reference points) are used, the applied force can be obtained. Some information about the shape of the object applying the force can also be obtained, but this is limited. One aspect, which complicates the analysis considerably, is the difference between d_{31} and d_{32}, as the output from the sensing element will vary according to the angle between the sensing element and the point force as well as the distance between them. These variations have been examined experimentally and are reported in Section 3.

3. Experimental measurements and results

Tests were conducted with a circular probe of 2-mm diameter and in addition with probes of various shapes and orientation. A signal generator drove the vibration unit, so that the probe applied a sinusoidal force to the sensor. The charge generated on the surface of the PVDF film (Good Fellow, England) was monitored by a charge amplifier (D.J. Birchal model o4, England) and displayed on a chart recorder. The magnitude of the applied force was determined by a force transducer located between the probe and the vibrator. The experimental setup is shown schematically in Fig. 3. The errors in measurement come firstly from the position of the centre of the probe on the intended points on the membrane. Considering the diameter of the probe, a possible mispositioning of 0.5 mm is estimated. This introduced a maximum error of 12%. Secondly, a possible 1-mm variation in extracting the peak values of the sinusoidal trace from the chart recorder was estimated; this introduced a further error of 5%. Non-uniform stretching of the membrane film was also possible, but the induced error is difficult to estimate.

3.1. Three-element membrane sensor

A circular 25-μm thick, uniaxially drawn (4:1 ratio) and unpoled film of PVDF was cut to a diameter of 100

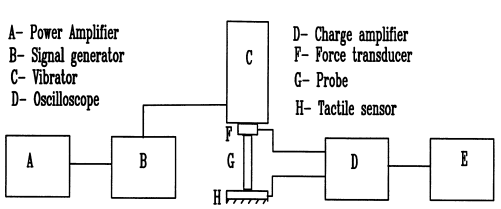

Fig. 3. Schematic diagram of the apparatus for experiments on the membrane system. Dynamic load is applied by the vibrator and the output charge from the PVDF sensing elements is measured by a charge amplifier and recorded on a chart recorder.

mm. Using masking plates on either side of the film, three rectangular-shaped aluminium electrodes of 2-mm width were deposited using the vacuum deposition method. The electrodes were arranged so that the intersection of two electrodes one on either side of the film formed a square sensor element. With this arrangement, the three elements formed a triangle in the centre of the PVDF Film. The film was then poled and tested for piezoelectric coefficients. Poling was carried out at 100°C with an applied voltage of 2 kV. With the voltage applied, the film was placed on a wooden substrate without any mechanical constrain and held at 100°C for 1 h, then allowed to cool to room temperature before the applied voltage was removed. The poling conditions, temperature and voltage, were not optimised. After the poling, the film was wrinkled slightly. Pinholing was also apparent in the specimen. This occurs when the film breaks down and the current though the film is sufficient to vapourise. Pinholing is attributable to imperfections in the film reducing the breakdown strength of the film. Current-limiting resistors were used in series with the film during poling. The angles of the triangle were divided into subdivisions of 10° and straight lines were drawn passing though the centre of each sensor element. Each line was marked at 4-mm intervals. The film was held between two 12-mm thick flat perspex plates, each with a 90-mm diameter centre hole. The plates were manufactured for precision fitting of the cup and cone-type arrangement, which helped to firmly hold and uniformly stretch the film, thus allowing the film to be replaced easily. The detailed construction of the sensor is shown in Fig. 4. An oscillatory force was applied at the marked points on the membrane, via a 2-mm diameter probe, away from the sensing elements. The stresses were transmitted to the sensing elements only by the membrane. This experiment was repeated for three different rubber supports of 12-mm thickness and elastic moduli of 2.4×10^4 Nm^{-2}, 3.3×10^4 Nm^{-2} and 1.05×10^5 Nm^{-2}.

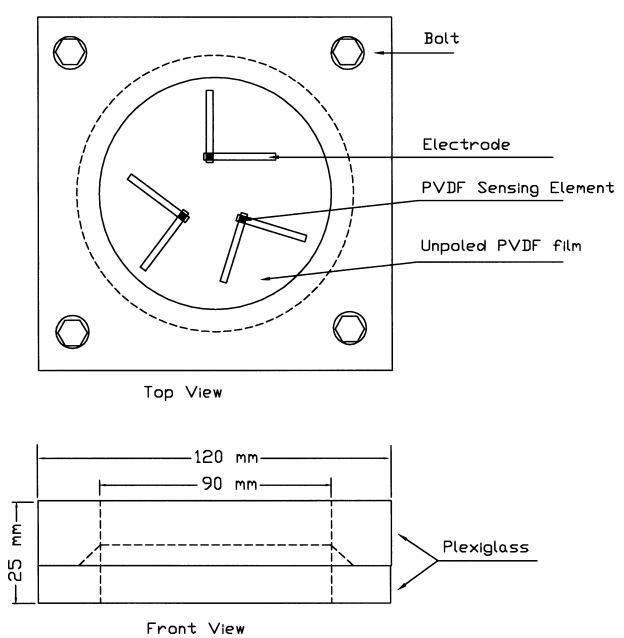

Fig. 4. The detailed construction of the three sensing-element membrane system. The area of overlap of the two electrodes, one on either side of the PVDF film, forms a sensing element.

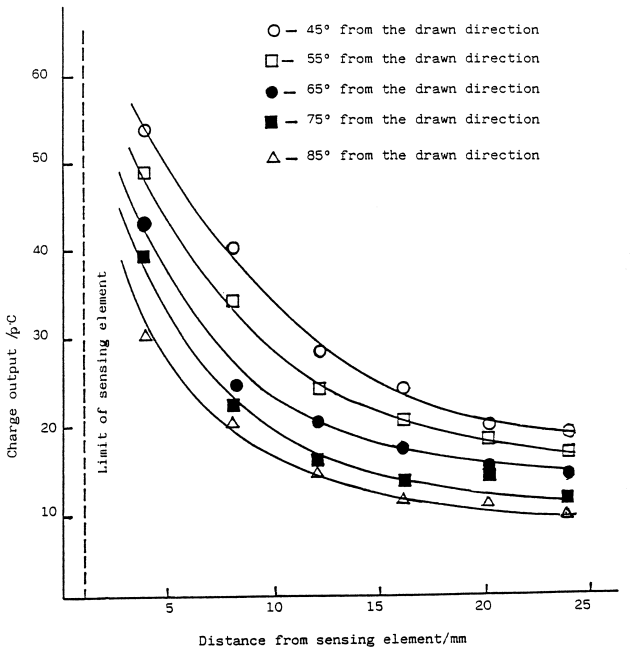

Fig. 5. The experimental results from one of the PVDF sensing elements (B), on the three-element sensor system with no rubber support. The response of the sensor decreases as the distance of the probe from the center of the sensing element increases and/or the angle between the line joining the center of the probe and sensing element and drawn direction of the film increases. Error for these experiments was estimated to be 17%.

In order to measure the angle of deflection of the membrane due to the application of the probe, a clock gauge was positioned below the membrane at the probe site. The average angle of deflection was calculated and found to be approximately 6°. This angle was used in the calculation of the theoretical output charge.

The results obtained showed that the output from each sensing element dropped rapidly with the distance of the applied force from the centre of the sensing element. This was particularly marked for one of the sensing elements for the unsupported membrane, where the output charge dropped off inversely proportional to the 0.8th power of distance from the sensing element. These results for the sensing element (B) are shown in Fig. 5. The results of all the other sensing elements with or without elastomer support indicated that the output charge varied inversely proportional to between 0.6 and 1 power of distance from the sensing elements. These results (not shown here), combined with the triangulation approach, are used to obtain the position of the applied force. Then the contours of the output charge versus distance away from the sensing ele-

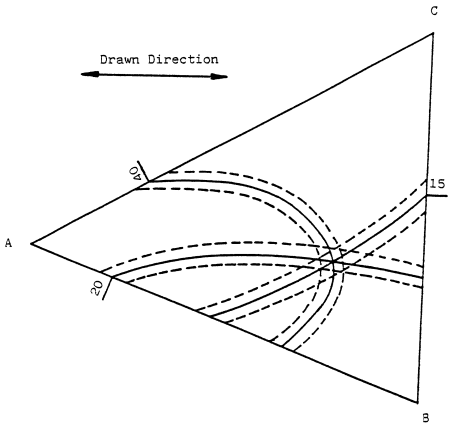

Fig. 6. Data extracted from all three sensing elements showing that the position of the three lines of output charge from the sensing elements represents the position of the probe on the plane of the PVDF membrane sensor. It also shows the 17% error bands associated with each contour.

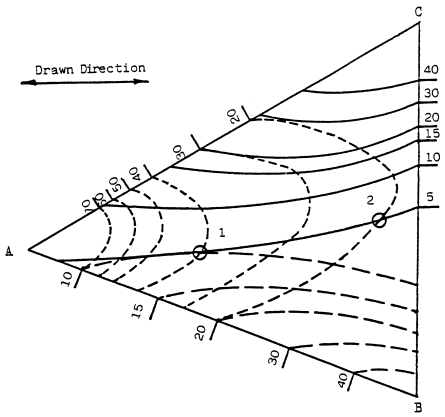

Fig. 8. Similar graph to that in Fig. 7 with rubber ($E = 3.3 \times 10^4$ Nm^{-2}) below membrane. The position of the probe at any point in the plane of the membrane is obtained by the point of intersection of contours from three sensing elements (1). Within the triangle ABC, only two contours are necessary for location of a point (2). The charge associated with contour line is measured in pico-coulombs.

ments for various positions of the probe for all three sensing elements are drawn. Utilising data from all three elements, the results for the unsupported membrane, showing the intersection of the output charge contours for the position of the applied force along with the associated error band, are shown in Fig. 6. The complete results for the unsupported membrane and the elastomer support ($E = 3.3 \times 10^4$ Nm^{-2}) are shown in Figs. 7 and 8, respectively.

In addition to position and force sensing, a number of experiments were conducted to determine whether or not the three-element sensor can distinguish between flat objects of various shapes and size. Hence, a second circular probe 14 mm in diameter was tested with the same experimental procedures as described above. The results did not show any significant difference in the output charge from each PVDF sensing element. This is because the experiments were conducted within the elastic limit of the PVDF film. Therefore, the stresses on the sensing elements are the same regardless of the probe used; consequently, the output charge also remains the same.

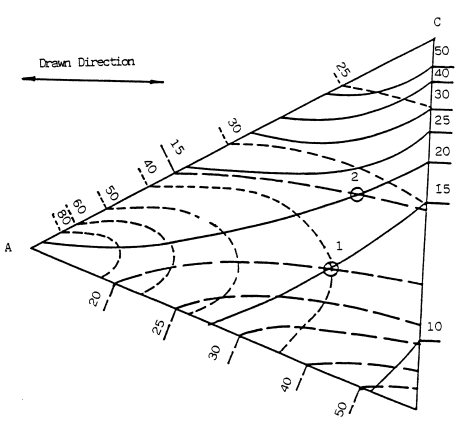

Fig. 7. Data extracted from all three sensing elements showing various contours of equal charge output. The position of the probe at any point in the plane of the membrane is obtained by the point of intersection of contours from three sensing elements (1). Within the triangle ABC, only two contours are necessary for location of a point (2). The charge associated with each contour line is measured in pico-coulombs.

Further experiments included the use of an equilateral triangle probe of 6.5-mm sides and rectangular probe of 7-mm length and 3 mm breadth, which were tested with the same procedure as described above. The results produced are similar to those for the 2-mm circular probe and show that the output charge reduces as the distance of the probe from the sensing element increases. It has also been observed that charge output increases as the angle between the drawn direction and the line joining the centroid of the probe and the centre of the sensing element increases.

In addition, these experiments show that when the triangular or rectangular probe were oriented differently (without changing the position of the centroid of the object), the output charge from each sensing element varied. Furthermore, when the vertex of the triangular probe or the short side of the rectangular probe was pointed directly towards the sensing element, at a given boundary distance from the sensing element, it exhibited much higher output charge than when either the base of the triangular probe, or the long side of the rectangular probe, was thus oriented.

4. Theoretical analysis

The 25-μm thick film used as a membrane sensor does not exhibit any flexural rigidity. When a force is applied at the centre of the PVDF membrane, the deflected shape will be conical. However, in the present experimental work with the three-point membrane sensing elements, the force was not always applied at the centre, but it was close to

centre. This means that the deflected conical shape can be assumed to be axisymmetric about the point of the applied force. The resultant radial force at any point of the membrane can be obtained from a simple equilibrium. Strictly, this will only be true for a membrane of infinite diameter; but the probe in these experiments was applied to the membrane within 12 mm of its centre so that deviations from the simplified theory are likely to be small (about 10%–15%), comparable to other errors arising in the measurements. The resultant radial force, $N\varphi$, is given by:

$$N\varphi = \frac{F}{2\pi r \sin(\alpha)}, \tag{6}$$

where α is the deflected angle of the membrane, F is the applied force and r is the distance of the probe away from sensing element.

The radial stress σ_r can thus be expressed as:

$$\sigma_r = \frac{F}{2\pi r t \sin(\alpha)}, \tag{7}$$

where t is the thickness of the film.

The stress in the deformed conical membrane is in the radial direction only, and the circumferential stress is negligible; this is because there is little or no expansion in the circumferential direction due to the applied force.

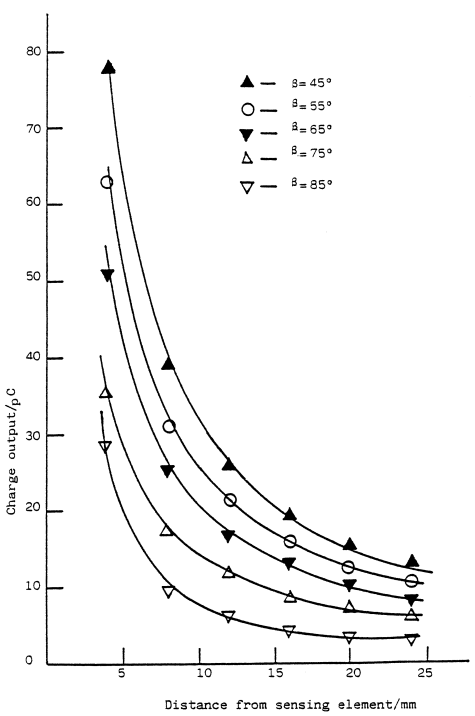

Fig. 9. The theoretical results for a PVDF sensing element on the three-element sensor system. The output charge decreases as the distance of the probe from the center of the sensing element increases and/or the angle between the line joining the center of the probe and the sensing element and the drawn direction of the film increases. The graph is obtained using Eq. (8) (see Section 4).

As the uniaxially drawn PVDF film is orthotropic, the value of the output charge, contributed by the piezoelectric constant d_{31} and d_{32}, is expressed as:

$$Q = (d_{31}\cos\beta + d_{32}\sin\beta)\sigma_r A_3, \tag{8}$$

where β is the angle between the drawn direction and the line connecting the position of the applied force with the centre of a sensing element; d_{31}, d_{32} and A_3 are defined at Eq. (2).

The variation of the output charge with the distance, r, of the probe away from the sensing element and the angle β is shown in Fig. 9. The graph shows that as the distance between the position of the applied force and the sensing element increases, the output charge decreases. In addition to that, as the angle β increases the output charge decreases. In these analyses, the value of α was 6°, which was experimentally obtained.

5. Discussion

The choice of the size of the diameter of each membrane was limited by the size of the drawn and unpoled PVDF film available in the market at the time of experiment.

The results obtained from the theoretical analysis Fig. 9 resemble the experimental ones Fig. 5. In both cases (experimental and theoretical), the output charge reduced as the distance, r, and the angle, β, increased. The experimental output charge varies inversely with the 0.6–1 power of distance away from the sensing element, while the theoretical analysis indicates that the output charge is proportional to the inverse of the distance from the sensing element. The lack of agreement between the theoretical and experimental results could be attributed both to the experimental errors and the assumptions in the theoretical analysis. For any magnitude of applied force (providing the force does not cause the film to exceed its elastic limit), the position of the applied force on the membrane can be uniquely determined. This means that with this method, both position and the magnitude of the applied force can be determined.

Using the membrane tactile sensing system demonstrated here, it has been shown that by using a flexible substrate, the entire polymer surface can be used to sense the force and its position with only three sensing elements. Because of the infinite number of contour lines which can be drawn, the entire surface of the membrane can be considered to be an active area. Here, the non-piezoelectrically active regions are mechanically active in transmitting stress to the sensing elements. This is in contrast to matrix tactile sensors where the areas between adjacent sensing elements are inactive. Another advantage of this sensor over the rigid substrate PVDF tactile sensor is its high sensitivity. Because the film is used as a membrane, the output charge is the sum of the charge due to piezoelectric

constants d_{31} and d_{32}, while in rigid substrate tactile sensors, it is effectively due to d_{33}. The output charge depends also on the applied force on the sensing element. The value of d_{31} and d_{32} are 6.5 pC/N and 0.65 pC/N, respectively, for the PVDF film used in these experiments.

The value of d_{33} would normally be greater than or equal to d_{31} [15]. It is reasonable to assume that $d_{33} = 10$ pC/N; therefore, the output charge from a sensing element due to application of say 0.25 N applied force for the rigid substrate system can be calculated using $Q = d_{33} \times F = 2.5$ pC. The same force on the membrane sensor, say 5 mm away from the sensing element and for $\beta = 45°$ will produce an output charge of 19 pC (see Eq. (3)); thus, the sensitivity is increased almost eight times. The piezoelectric constants determined for the sensing elements were three times lower than the manufacturer quoted; however, with improved poling conditions (i.e., by optimising poling conditions, higher temperature and voltage), much higher sensitivity could be achieved.

The results of the experiments on various probe shapes suggest that the membrane is distorted according to the different shape or orientation of the object. This is because differently shaped boundaries cause different output charges from the sensing element. This may be explained in that, as the boundary shape becomes narrow, for a given applied force, it causes higher local distribution, thus higher strain and consequently, higher output charge from the sensing element. In order to obtain the position of different flat-shaped probes (i.e., triangular or rectangular), at least four sensing elements are required. The triangulation of each set of three sensing elements would give a different nominal centroid position. This is because of the variation in the output charge with the difference in shape of the boundary. The average value of the coordinates will then give a more accurate position for the centroid of the flat probe. Once the position of the centroid of the probe is obtained, it is possible to find some information about the shape of the object/probe. This is done by considering the output charge from each individual sensing element. If, however, the number of sensing elements is increased, that is, 5, 6, etc., more information about the shape of the boundary of the probe/object can be obtained. The limitation of this approach is that it is based on boundary recognition, and thus if the probe has say, a central hole, this sensor cannot distinguish from a probe with a solid centre.

In addition to robotic tactile sensing, the sensor can also be used in both minimally invasive surgery using endoscopic tools [16,17,19,21] and in prosthetic hands [22–24] for grasping tissues/objects. In the former, the output from the sensor is often fed back to the surgeon's finger via various pins [25]. A reduction in the number of sensing elements will reduce the resolution of the surgeon's perception, thus limiting the complexity of the operation. In the latter, the signals from a sensor on the prosthetic finger are often fed to that part of the body which has tactile sensitivity (such as the chest region); again the reduction in the number of sensing points will reduce the dexterity with which a prosthetic hand can manipulate objects.

References

[1] A.S. Fiorillo, P. Dario, M. Bergamasco, Sensorized robot gripper, Robotics (Netherlands) 4 (1) (1988) 49–55.

[2] D.G. Pirolo, E.S. Kolesar, Piezoelectric polymer tactile sensor array for robotics, Proc. IEEE Natl. Aerospace and Electronics Conf., Dayton, 3, NJ, USA, 22–26 May 1989, pp. 1130–1135.

[3] R.R. Reston, E.S. Kolesar, Robotic tactile sensor array fabricated from a piezoelectric polyvinylidene fluoride film, Proc. IEEE Natl. Aerospace and Electronics Conf., 3, Dayton, USA, 21–25 May 1990, pp. 1139–1144.

[4] P. Dario, R. Bardelli, D. De Rossi, L.R. Wang, P.C. Pinotti, Touch-sensitive polymer skin uses piezoelectric properties to recognise orientation of objects, Sensor Review 2 (4) (1982) 194–198.

[5] P. Dario, D. De Rossi, C. Domenici, R. Francesconi, Ferroelectric polymer tactile sensor with anthropomorphic features, Proc. IEEE Int. Conf. on Robotics, Atlanta, GA, USA, 1984, pp. 332–340.

[6] P. Dario, M. Bergamasco, A. Fiorillo, R. Dlleonardo, Geometrical optimisation criteria for the design of tactile sensing patterns, Proc. IEEE Int. Conf. on Robotics and Automation, San Francisco, USA, 7–10 Apr. 1986, pp. 1268–1273.

[7] P. Dario, M. Bergamasco, D. Femi, A. Fiorillo, A. Vaccarelli, Tactile perception in unstructured environments: a case for rehabilitation robotics applications, Proc. IEEE Int. Conf. on Robotics and Automation, Raleigh, NC, USA, 31 Mar. 1987, pp. 2047–2054.

[8] H. Shinoda, S. Ando, Tactile sensors with 5-D deformation sensing element, Proc. IEEE Int. Conf. on Robotics and Automation, 1, 1996, pp. 7–12.

[9] R. Lazzarini, R. Magni, P. Dado, Tactile array sensor layered in an artificial skin, Proc. IEEE Int. Conf. on Intelligent Robots and Systems, 3, USA, 1995, pp. 114–119.

[10] J.S. Son, E.A. Monteverde, R.D. Howe, Tactile sensor for localizing transient events in manipulation, Int. Conf. on Robotics and Automation, 1, USA, 1994, pp. 471–476.

[11] Y. Jiar, K. Lee, G. Shi, High resolution and high compliance tactile sensing system for robotic manipulations, Int. Conf. on Intelligent Robot System, Yokohama, Japan, 1993, pp. 1005–1009.

[12] P. Dario, G. Buttazzo, Anthropomorphic robotic finger for investigating artificial tactile perception, Int. J. Robotics Res. 6 (3) (1987) 24–48.

[13] E.S. Kolesar, P.R. Reston, D.G. Ford, R.C. Fitch, Multiplexed piezoelectric polymer tactile sensor, J. Robotic Systems 9 (1) (1992) 37–63.

[14] E.S. Kolesar, C.S. Dyson, R.R. Reston, R.C. Fitch, D.G. Ford, S.D. Nelms, Detecting low-intensity magnetic fields with a magnetostrictive fibre optic sensor, Proc. of the Annual IEEE Int. Conf. on Innovative Systems in Silicon, 1996, pp. 372–381.

[15] J. Dargahi, Application of polyvinylidene fluoride as a robotic tactile sensor, PhD Thesis, Glasgow Caledonian University, Glasgow, UK, Apr. 1993.

[16] F. Tendick, T. Mori, L. Way, The future of laparoscopic surgery, in: L. Way, S. Bhoyrul, T. Mori (Eds.), Fundamentals of Laparoscopic Surgery, Churchill-Livingston, 1995.

[17] A. Bicchi, G. Canepa, D. De Rossi, P. Iacconi, E.P. Scilingo, A Sensorized minimally invasive surgery tool for detecting tissutal elastic properties, Proc. IEEE Int. Conf. on Robotics and Automation, Minneapolis, MN, April 1996.

[18] E.S. Kolesar, Piezoelectric micromechanical sensor array capable of generating three dimensional tactile images, Proc. of the 1997 43rd Int. Instrumentation Symposium, Orlando, FL, USA, 4–8 May 1997.

[19] J. Dargahi, S. Payandeh, Surface texture measurement by combining signals from two sensing elements of a piezoelectric tactile sensor,

Proc. SPIE Int. Conf. on Aerospace/Defense Sensing, Simulation, and Controls, 3376, Orlando, FL, USA, 13–17 April 1998.
[20] T.T. Wang, J.M. Herbert, A.M. Glass (Eds.), The Applications of Ferroelectric Polymers, Blackie, New York, 1988.
[21] J. Dargahi, M. Parameshwaran, S. Payandeh, A micromachined piezoelectric tactile sensor for use in endoscopic grasper, IEEE/RSJ Int. Conf. on Intelligent Robots and Systems, Victoria, BC, Canada, October 1998.
[22] G.F. Shannon, Sensory feedback for artificial limbs, Med. Prog. Technol. 6 (2) (1979) 73–79.
[23] G.F. Shannon, P.J. Agnew, Fitting below-elbow prostheses which convey a sense of touch, Med. J. 1 (6) (1979) 242–244.
[24] P.J. Agnew, G.F. Shannon, Training for a myo-electrically controlled prosthetics with sensory feedback system, Am. J. Occup. Ther. 35 (11) (1981) 722–727.
[25] R.D. Howe, W.J. Peine, D.A. Kontarinis, J.S. Son, Remote palpation technology, Proc. IEEE Int. Conf. in Medicine and Biology, May/June 1995.
[26] P.E. Crago, R.J. Nakai, H.J. Chizeck, Feedback regulation of hand grasp opening and contact force during simulation of paralysed muscle, IEEE Trans. Biomed. Eng. 38 (1) (1991) .

J. Dargahi completed his BSc, MSc and PhD degrees in the United Kingdom. He was employed as a research assistant in Glasgow Caledonian University in Scotland and as an Assistant professor in Amirkabir University of Technology in Iran. He was then employed as a senior research associate in Micromachining/Medical Robotic group at Simon Fraser University in British Columbia. He is now working as a lecturer at the University of New Brunswick in Saint John, Canada.